

# Impact of Disease on Plasma and Lung Exposure of Chloroquine, Hydroxychloroquine and Azithromycin: Application of PBPK Modeling

Karen Rowland Yeo<sup>1,\*</sup>, Mian Zhang<sup>1</sup>, Xian Pan<sup>1</sup>, Alice Ban Ke<sup>1</sup>, Hannah M. Jones<sup>1</sup>, David Wesche<sup>2</sup> and Lisa M. Almond<sup>1</sup>

We use a mechanistic lung model to demonstrate that accumulation of chloroquine (CQ), hydroxychloroquine (HCQ), and azithromycin (AZ) in the lungs is sensitive to changes in lung pH, a parameter that can be affected in patients with coronavirus disease 2019 (COVID-19). A reduction in pH from 6.7 to 6 in the lungs, as observed in respiratory disease, led to 20-fold, 4.0-fold, and 2.7-fold increases in lung exposure of CQ, HCQ, and AZ, respectively. Simulations indicated that the relatively high concentrations of CQ and HCQ in lung tissue were sustained long after administration of the drugs had stopped. Patients with COVID-19 often present with kidney failure. Our simulations indicate that renal impairment (plus lung pH reduction) caused 30-fold, 8.0-fold, and 3.4-fold increases in lung exposures for CQ, HCQ, and AZ, respectively, with relatively small accompanying increases (20 to 30%) in systemic exposure. Although a number of different dosage regimens were assessed, the purpose of our study was not to provide recommendations for a dosing strategy, but to demonstrate the utility of a physiologically-based pharmacokinetic modeling approach to estimate lung concentrations. This, used in conjunction with robust *in vitro* and clinical data, can help in the assessment of COVID-19 therapeutics going forward.

## Study Highlights

### WHAT IS THE CURRENT KNOWLEDGE ON THE TOPIC?

✓ Several publications have recently appeared relating to the application of physiologically-based pharmacokinetic models for prediction of the exposure of chloroquine (CQ) and hydroxychloroquine (HCQ) in lung and plasma. Both drugs have been identified as potential candidates for treatment of coronavirus disease 2019 (COVID-19).

### WHAT QUESTION DID THIS STUDY ADDRESS?

✓ We sought to demonstrate that a modeling approach can be used to assess the effects of physiological changes, potentially evoked by COVID-19, on the plasma and lung exposure of CQ, HCQ, and azithromycin (AZ).

### WHAT DOES THIS STUDY ADD TO OUR KNOWLEDGE?

✓ We confirm that the accumulation of CQ, HCQ, and AZ in the lungs is very sensitive to changes in pH, a parameter that could be affected by COVID-19. We also demonstrate that renal impairment, a comorbid condition of COVID-19, may lead to increased concentrations of all three drugs in the lungs.

### HOW MIGHT THIS CHANGE CLINICAL PHARMACOLOGY OR TRANSLATIONAL SCIENCE?

✓ The approach and mechanistic lung model described here could be applied to other drugs being investigated as COVID-19 therapeutics.

Coronavirus disease 2019 (COVID-19) has rapidly become a global pandemic, since the outbreak was initially identified in Wuhan, China, in December 2019. The virus, severe acute respiratory syndrome coronavirus 2 (SARS-CoV-2), can infect the lower respiratory tract causing fevers, cough, and pneumonia. As new drug candidates are being investigated for treatment of COVID-19, efforts are being made to repurpose existing antimicrobial drugs, as they are readily available, and have a known safety

profile. Specifically, it has been reported that chloroquine (CQ) has been successful in treating SARS-CoV-2 infections in China.<sup>1</sup> *In vitro* studies have since confirmed that hydroxychloroquine (HCQ), an analog of CQ, is a more potent inhibitor of SARS-CoV-2 (5-fold to 7-fold).<sup>2</sup> Given that HCQ also has a more favorable safety profile than CQ during chronic dosing, a clinical study was conducted in France to determine whether HCQ (600 mg daily; 465 mg base) could be a more viable option for COVID-19

<sup>1</sup>Certara UK Limited (Simcyp Division), Sheffield, UK; <sup>2</sup>Certara Inc., Princeton, New Jersey, USA. \*Correspondence: Karen Rowland Yeo ([Karen.Yeo@certara.com](mailto:Karen.Yeo@certara.com))

Received April 22, 2020; accepted June 6, 2020. doi:10.1002/cpt.1955

treatment.<sup>3</sup> Despite its small sample size, the results of the study showed that treatment with HCQ alone or in combination with azithromycin (AZ) shortened the time to resolution of viral shedding. Based on the results of this study, clinicians in many countries have already begun using these medications in clinical practice, and multiple randomized trials are being initiated.

For effective treatment of viral pneumonia in the lungs, it is expected that the concentration of drug at the site of infection should achieve or exceed effective concentration 90% ( $EC_{90}$ ) values for inhibition of SARS-CoV-2. Uptake of drugs into the lungs is particularly significant for basic amines, such as CQ, HCQ, and AZ, with  $pK_a$  values > 8. Most basic amines, including CQ and HCQ, are amphiphilic, with a large hydrophobic group and a hydrophilic group that is ionized at physiological pH.<sup>4</sup> This makes them susceptible to lysosomal trapping, a mechanism that can lead to significant accumulation of a drug in the lungs, or other lysosomal rich organs, such as the heart.<sup>5</sup> Small changes in the pH of the lungs as a consequence of a SARS-CoV-2 infection may, therefore, have a significant impact on the accumulation of CQ, HCQ, and AZ in lung tissue or the epithelial lining fluid (ELF) relative to plasma.

Most of the published articles on COVID-19 have focused on the lungs as the main organ involved in the disease, whereas few articles have reported SARS-CoV-2 involvement in other organs, including liver and kidneys, both of which are involved in the metabolism and excretion of CQ, HCQ, and AZ. Liver injury and an increased incidence of acute renal injury during SARS-CoV-2 infection have been reported.<sup>6,7</sup> This is likely to add to the complication of deciding on the correct therapeutic dose of CQ, HCQ, and AZ in patients with COVID-19 and may lead to an increased risk of adverse drug reactions. Physiologically-based pharmacokinetic (PBPK) modeling allows integration of drug-related data (absorption, metabolism, plasma protein binding, and physicochemical) with relevant physiology, to simulate profiles of drug in plasma as well as other organs and tissues, including the site of action.<sup>8</sup> Thus, changes in physiology as a consequence of disease can be assessed using PBPK modeling, including renal<sup>9</sup> and hepatic impairment.<sup>10</sup>

Two recent publications have applied PBPK modeling to predict the exposure of HCQ and/or CQ in the lungs.<sup>2,11</sup> In the first of these publications, Yao *et al.*<sup>2</sup> applied a lung to plasma partition coefficient ( $K_p$ ) of 541 for HCQ based on rat data and then compared the significantly enhanced lung exposure with an *in vitro* derived half-maximal effective concentration ( $EC_{50}$ ). Arnold and Buckner<sup>11</sup> reported on the limitations of the former study, mainly focusing on the source of the  $K_p$  value and the fact that the lung concentrations were referenced against an  $EC_{50}$  rather than an  $EC_{90}$ . The authors assessed the impact of a range of  $K_p$  values (including other rat studies— $K_p$  of 220) on the lung exposure for a number of different dosing regimens for HCQ and concluded that improved PK models were required for HCQ in order to have more confidence in the efficacy of HCQ against SARS-CoV-2.

We use previously published PBPK models for CQ, HCQ, and AZ, and integrate a more mechanistic permeability-limited lung model,<sup>12</sup> which allows us to investigate the exposure of the drugs in lung tissue and ELF, rather than considering the lung as a homogeneous perfusion-limited organ, as in previous publications.<sup>2,11</sup> We also assess the impact of COVID-19 (via potential pH changes in

the lung and renal impairment as a covariate) on the accumulation of each of the drugs in the plasma and lungs. In addition, we compare the predicted exposure of each drug in plasma and lungs with the published  $EC_{50}$  and  $EC_{90}$  values.

## METHODS

### *In vitro* $EC_{50}$ values

A literature search was conducted to collate  $EC_{50}$  values for CQ, HCQ, and AZ determined *in vitro*. It was noted that the *in vitro* viral activity assays differed slightly in their methodology where described in detail. However, in essence, Vero E6 cells were maintained in medium supplemented with low levels of serum and infected with SARS-CoV-2 virus at a multiplicity of infection ranging from 0.001–0.8 for several hours at a temperature of 37°C. These virus cells were then washed with media and treated with medium containing drug over a range of concentrations for 24 or 48 hours. Viral RNA was extracted and analyzed by Real-Time polymerase chain reaction. In each of the publications, a sigmoidal Hill function was used to estimate  $EC_{50}$  values (half maximal viral inhibition constant).<sup>2,13–15</sup>

### Effect of COVID-19 on lung pH and other key physiological parameters

A survey of literature data was performed to identify parameters, such as plasma binding proteins and pH values for the lung tissue and ELF that may influence the predicted systemic and lung drug exposures in a “COVID-19 population.” Due to the scarcity of data specific for COVID-19, we expanded our search to other types of viral pneumonia (Supplementary Information).

### Simulations using full PBPK and the permeability limited lung model

The Simcyp (version 19.1) population-based PBPK simulator (Simcyp, Sheffield, UK) was used to generate the profiles of CQ, HCQ, and AZ. PBPK models for all three compounds were verified and published previously.<sup>2,16</sup> Each of these models was refined to include a permeability-limited lung model.<sup>12</sup> Based on its anatomy and physiology, the lung model is described by seven segments representing upper and lower airways (2 segments) and the lobes of the lungs (5 segments). Each segment is divided into four compartments representing pulmonary capillary blood, tissue mass, fluid, and alveoli air. The fluid compartment represents mucus and ELF (pH = 6.6), whereas the mass compartment represents the different cell types within the lungs (pH = 6.7).

For each compound, Henry's constant was predicted using a quantitative structure–activity relationship approach and used to calculate the air:fluid partition coefficient. Three different *in vitro-in vivo* extrapolation approaches are available to predict lung permeability. The preferred method is *in vitro* permeability data obtained from the Calu-3 cell line.<sup>12</sup> However, Caco-2 permeability data ( $P_{app}$ ) or physicochemical properties, such as Log D,  $pK_a$ , hydrogen bond donor count can be used to predict Calu-3 permeability and, hence, lung permeability. The *in vitro* permeability data are corrected by the unionized fraction of compound (calculated at the pH of the *in vitro* system) as only the unbound, unionized drug is considered to be passively permeable in the lung PBPK model. Due to low protein concentrations in ELF,<sup>17</sup> the unbound fraction in the ELF was assumed to be one for all three drugs. Measured values of unbound fraction in lung tissue homogenate ( $f_{u, \text{mass}}$ ) could not be found for any of the compounds, therefore,  $f_u$  in lung tissue mass was predicted as reported previously.<sup>18,19</sup>

After integrating the permeability-limited lung model, simulations were run to assess the impact of key physiological parameters (pH in the lung) on the exposure of each of the drugs in the lungs and plasma using a number of different dosage regimens that are currently being assessed in clinical trials. The effect of severe renal impairment (glomerular filtration rate (GFR) < 30 mL/min) was assessed using the population (elevated AAG, reduced albumin levels, and elevated serum creatinine) within the

Simcyp Simulator. Unless stated otherwise, 100 subjects aged 20–80 years (50% men and 50% women) were simulated.

For all of the above scenarios, the simulated concentrations for total lung, unbound lung, total ELF (assumed to be the same for unbound), and total plasma were compared against the lowest and highest reported  $EC_{50}$  values. In addition, trough lung concentrations (unbound) were compared against a reported or extrapolated  $EC_{90}$  ( $9 \times EC_{50}$ ).

### Chloroquine

The input parameters for the CQ model are provided in **Supplementary Supporting Material Table S1** and **Table S2**. An *in vitro* Caco-2  $P_{app}$  value of  $21 \times 10^{-6}$  cm/s was used to predict permeability across the lungs.<sup>20</sup> Henry's constant was predicted to be  $1.08 \times 10^{-7}$  Pa m<sup>3</sup>/mol (EPI Suite). Simulations were performed to demonstrate that the updated CQ model was able to generate concentration-time profiles that were consistent with observed data (**Supplementary Information**). Predicted lung exposures relative to plasma over time were generated for a single 300 mg CQ dose and the Kp values were compared with observed rat data. The effect of lung pH (5.5–6.7) on the Kp values was also assessed.

Plasma and lung exposures were simulated for different dosage regimens that have traditionally been used for malaria treatment or are currently being investigated for treatment of COVID-19. These include:

- 600 mg CQ base on days 1 and 2, and 300 mg on day 3 (1.5 g over 3 days) – World Health Organization (WHO) regimen.
- 600 mg CQ base on day 1 at 9 AM, followed by 300 mg at 3 PM on day 1, followed by 300 mg at 9 AM on days 2 and 3 (1.5 g over 3 days) – US Food and Drug Administration (FDA) regimen.
- 1,200 mg CQ base on day 1 followed by 300 mg q.d. for 9 days (3.9 g over 10 days) (ClinicalTrials.gov Identifier: NCT04328493).
- 600 mg CQ base b.i.d. for 10 days (12 g over 10 days) (ClinicalTrials.gov Identifier: NCT04323527).

E. 300 mg CQ base q.d. for 4 days, followed by 300 mg weekly out to 30 days (1.65 g over 30 days) (ClinicalTrials.gov Identifier: NCT04333732).

F. 300 mg CQ base q.d. for 4 days, followed by 150 mg q.d. out to 30 days (5.1 g over 30 days) (ClinicalTrials.gov Identifier: NCT04333732).

### Hydroxychloroquine

With the exception of a metabolic intrinsic clearance of 21.5  $\mu$ L/min/mg protein, the input parameters for the HCQ model were as cited previously by Yao *et al.*<sup>2</sup> An *in vitro* Caco-2  $P_{app}$  value of  $0.138 \times 10^{-12}$  cm/s (50-fold lower than that of CQ based on Ferrari *et al.*<sup>21</sup>) was used to predict permeability across the lungs. Henry's constant was predicted to be  $3.98 \times 10^{-12}$  Pa m<sup>3</sup>/mol (EPI Suite; **Table S1**). Plasma and lung exposures were simulated for the dosage regimen used in the French study; 200 mg HCQ (155 mg base) was given every 8 hours for 10 days.<sup>3</sup>

### Azithromycin

With the exception of the B:P ratio, which was set at 2.28, the input parameters for the AZ model were as cited previously by Johnson *et al.*<sup>16</sup> An *in vitro* Caco-2  $P_{app}$  value of  $1.67 \times 10^{-6}$  cm/s calibrated using a  $P_{app}$  of  $10.4 \times 10^{-6}$  cm/s for propranolol<sup>22</sup> was used to predict permeability across the lungs. Henry's constant was predicted to be  $5.37 \times 10^{-24}$  Pa m<sup>3</sup>/mol (EPI Suite; **Table S1**). Simulations were performed to demonstrate that the updated AZ model was able to generate exposures of AZ that were consistent with observed data. Plasma and lung exposures were simulated for the dosage regimen used in the French study; 500 mg was given on day 1 followed by 250 mg once daily for 4 days.<sup>3</sup>

## RESULTS

### *In vitro* $EC_{50}$ values

Depending on the methodology applied, at 48 hours,  $EC_{50}$  values for CQ range between 1.13 and 7.36  $\mu$ M (**Table 1**). At 48 hours,

**Table 1** *In vitro*  $EC_{50}$  potency measures

Drug	Virus	Viral input MOI	Incubation time		$EC_{50}$ $\mu$ M	Source
			hour	hour		
CQ	SARS-CoV-2 Vero	0.01	48	48	5.47	Yao <i>et al.</i> <sup>2</sup>
CQ	SARS-CoV-2 Vero	0.01	24	24	23.9	Yao <i>et al.</i> <sup>2</sup>
CQ	2019-nCoV Vero E6	0.05	48	48	1.13	Wang <i>et al.</i> <sup>15</sup>
CQ	SARS-CoV-2 Vero E6	0.01	48	48	2.71	Liu <i>et al.</i> <sup>13</sup>
CQ	SARS-CoV-2 Vero E6	0.02	48	48	3.81	Liu <i>et al.</i> <sup>13</sup>
CQ	SARS-CoV-2 Vero E6	0.2	48	48	7.14	Liu <i>et al.</i> <sup>13</sup>
CQ	SARS-CoV-2 Vero E6	0.8	48	48	7.36	Liu <i>et al.</i> <sup>13</sup>
HCQ	SARS-CoV-2 Vero	0.01	48	48	0.72	Yao <i>et al.</i> <sup>2</sup>
HCQ	SARS-CoV-2 Vero	0.01	24	24	6.14	Yao <i>et al.</i> <sup>2</sup>
HCQ	SARS-CoV-2 Vero E6	0.01	48	48	4.51	Liu <i>et al.</i> <sup>13</sup>
HCQ	SARS-CoV-2 Vero E6	0.02	48	48	4.06	Liu <i>et al.</i> <sup>13</sup>
HCQ	SARS-CoV-2 Vero E6	0.2	48	48	17.31	Liu <i>et al.</i> <sup>13</sup>
HCQ	SARS-CoV-2 Vero E6	0.8	48	48	12.96	Liu <i>et al.</i> <sup>13</sup>
HCQ	SARS-CoV-2 Vero E6	0.001	48	48	4.17	Touret <i>et al.</i> <sup>14</sup>
AZ	SARS-CoV-2 Vero E6	0.001	48	48	2.12	Touret <i>et al.</i> <sup>14</sup>

AZ, azithromycin; CQ, chloroquine;  $EC_{50}$ , half-maximal effective concentration; HCQ, hydroxychloroquine; MOI, multiplicity of infection; nCoV, novel coronavirus; SARS-CoV-2, severe acute respiratory syndrome coronavirus-2.

$EC_{50}$  values for HCQ range between 0.72 and 17.3  $\mu\text{M}$ . A single  $EC_{50}$  value of 2.12  $\mu\text{M}$  was available for AZ. In each case, these represent total  $EC_{50}$  values as no protein binding corrections have been applied. However, given that the  $f_{u,p}$  values for CQ, HCQ, and AZ are 0.4, 0.5, and 0.69, respectively, it is expected that the protein binding in these *in vitro* pharmacology experiments will be minimal.

### Physiological parameters affected by COVID-19

Normal ELF pH is considered to be acidic, averaging  $\sim 6.6$  (range 5.7–7.5) in healthy airways compared with a blood and interstitial pH of 7.4. There are indications that in airway diseases, such as cystic fibrosis and pneumonia, ELF pH is more acidic, suggesting breakdowns in the pH regulatory mechanisms.<sup>23</sup> Using a pH electrode/probe, the most acidic measured pH value in ELF of bacterially infected pneumonia patients is 5.6. Another study indicated that the pH of exhaled breath condensate, which reflects the pH of the lining fluid of the lung, was lower in mechanically ventilated patients compared with spontaneously breathing individuals (mean  $\pm$  SD values of  $5.86 \pm 0.32$  vs.  $7.47 \pm 0.48$ ).<sup>24</sup> In the absence of human data describing the pH value for lung mass, a value of 6.69 based on experimental data obtained in dogs (ref. 25; range 6.46–6.97) is used in the model. Based on these data, the range for sensitivity analysis on lung mass pH in the current study was set to 6.0–6.7.

Serum albumin is commonly measured as part of the initial evaluation of critically ill patients with infectious disease. Several studies show that the frequency of hypoalbuminemia at admission is high in hospitalized patients with community acquired pneumonia.<sup>26</sup> The leading causes of hypoalbuminemia are malnutrition, reduced hepatic synthesis, renal losses, and inflammation; however, the predominant mechanism by which serum albumin decreases is secondary to increased capillary permeability and redistribution from plasma to the interstitium in critically ill patients.<sup>27</sup> A summary of serum albumin levels in differing types of viral pneumonia in the literature is presented in **Table S3**. The weighted mean albumin levels in severe cases of viral pneumonia is 29.3 g/L. Concentrations of an inflammation marker, AAG, are generally believed to increase during an infection, however, quantitative information is limited in patients with viral pneumonia. A 1.7-fold to 3-fold increase in AAG levels in patients with community-acquired pneumonia<sup>28</sup> or SARS-CoV<sup>29</sup> has been reported. As the above parameters appear to be reasonably consistent with those previously cited for patients with severe renal impairment,<sup>9</sup> they were accounted for in simulations of virtual patients with GFR  $< 30$  mL/min.

### Simulated plasma and lung exposure of CQ

The predicted  $K_p$  values for lung after a single oral dose of 300 mg CQ base are shown in **Figure 1**. Observed data in humans are not available for comparison and rat data from several different studies are presented. The predicted  $K_p$  value after 10 days ( $K_p = 166$ ) appears to be reasonably consistent with the rat  $K_p$  values ( $\sim 220$ ) that have been previously published by McChesney *et al.*<sup>30</sup> Of particular importance, is the finding that the predicted  $K_p$ , and hence the exposure in the lungs, is very sensitive to small changes

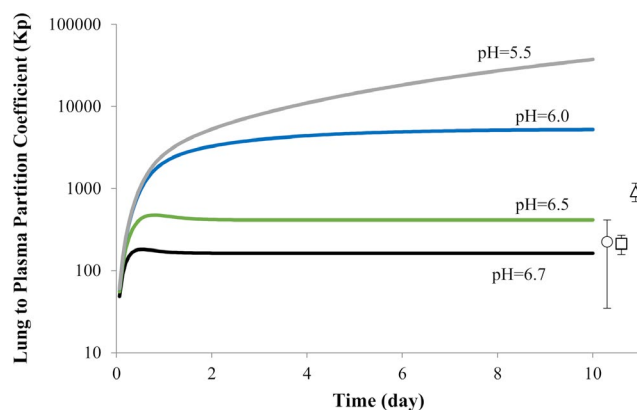


**Figure 1** Effect of lung pH on the lung to plasma partition coefficient ( $K_p$ ) over time after a single oral dose of 300 mg chloroquine base. The data points and error bars represent the mean and SD of the reported  $K_p$  values in rats (circle: Adelusi and Salako (1982a)<sup>36</sup>; square: Adelusi and Salako (1982b)<sup>37</sup>; triangle: McChesney (1967)<sup>30</sup>).

in pH. Indeed, a reduction in pH from 6.7 to 6.5 or down to 6.0, results in an increase in predicted  $K_p$  from 166 to 412 and 5,208, respectively.

The simulated concentration-time profiles for CQ in plasma and lung (lung tissue and ELF) based on various different dosage regimens are shown in **Figure 2**. When comparing the unbound lung exposure of CQ against the minimum cited  $EC_{50}$  value for inhibition of SARS-CoV-2, all dosage regimens appear to generate high enough exposures from the first day of dosing. However, when compared against the  $EC_{90}$  value (6.9  $\mu\text{M}$ ), the only dosage regimen that meets this target on day 1 is 600 mg b.i.d. for 10 days (**Table 2**). For two of the dosage regimens, the effect of reducing lung pH to six (lung tissue and ELF) and renal impairment are shown in **Figure 3**. Although the increase in CQ lung exposure is more sensitive to changes in pH than the added complication of renal impairment (protein binding and GFR), the combined effect resulted in 50-fold to 100-fold increases relative to the control scenario (lung pH = 6.7 and normal GFR; **Table 2**).

### Simulated plasma and lung exposure of HCQ

Simulated plasma exposures of HCQ after dosing of 400 mg (310 mg base) daily for 24 weeks were 1,700 ng/mL, which were reasonably consistent with observed values of about 1,400 ng/mL (data not shown; ref. 31). Concentration-time profiles for HCQ in plasma and lungs (lung tissue and ELF) following dosing of 200 mg (155 mg base) every 8 hours for 10 days are shown in **Figure 4**. The predicted  $K_p$  value of 243 after 10 days appears to be reasonably consistent with rat  $K_p$  values ( $\sim 220$ ) that have been previously published.<sup>30</sup> The change in lung pH does not result in a change in plasma exposure but does lead to a 4-fold increase in peak plasma concentration ( $C_{max}$ ) in the lung (179 vs. 710  $\mu\text{M}$ ). A 30% increase in plasma exposure is predicted in subjects with renal impairment and the  $C_{max}$  in the lungs is further increased to 1,492  $\mu\text{M}$ . Unbound lung concentrations of HCQ attain the

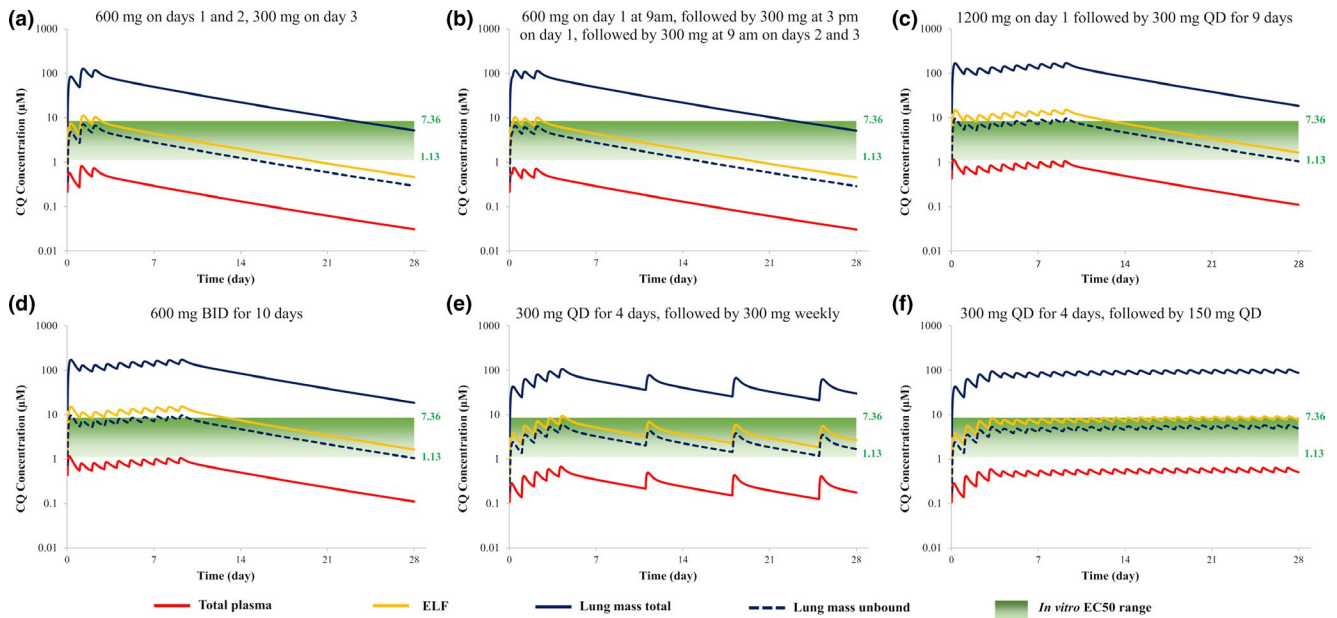


**Figure 2** Simulated plasma and lung concentrations of chloroquine (CQ) relative to *in vitro* half-maximal effective concentration (EC<sub>50</sub>) values for various dosing regimens. Total plasma (red line), lung mass total (blue solid line), lung mass unbound (blue dashed line), epithelial lining fluid (ELF; yellow line) are shown. (a) There was 600 mg administered on days 1 and 2, 300 mg on day 3 – World Health Organization (WHO) regimen; (b) 600 mg on day 1 at 9 AM, followed by 300 mg at 3 PM on day 1, followed by 300 mg at 9 AM on days 2 and 3 – US Food and Drug Administration (FDA) regimen; (c) 1,200 mg on day 1 followed by 300 mg q.d. for 9 days (ClinicalTrials.gov Identifier: NCT04328493); (d) 600 mg b.i.d. for 10 days (ClinicalTrials.gov Identifier: NCT04323527); (e) 300 mg q.d. for 4 days, followed by 300 mg weekly (ClinicalTrials.gov Identifier: NCT04333732); (f) 300 mg q.d. for 4 days, followed by 150 mg q.d. (ClinicalTrials.gov Identifier: NCT04333732).

**Table 2** Impact of lung pH and renal impairment on the lung CQ levels relative to *in vitro* efficacy (EC<sub>90</sub>) for different dosage regimens

No.	Study	Lung mass pH	R <sub>EC50</sub> , R <sub>EC90</sub> Days after the first dose			
			1	3	10	25
1	WHO regimen	6.7	2.4, 0.4	4.4, 0.7	1.9, 0.3	0.3, 0.1
2	FDA regimen	6.7	3.9, 0.6	4.3, 0.7	1.9, 0.3	0.3, 0.1
3	NCT04328493	6.7	4.8, 0.8	5.0, 0.8	6.8, 1.1	1.3, 0.2
4	NCT04323527	6.7	6.1, 1.0	5.0, 2.1	6.8, 4.1	1.3, 0.7
		6.0	54, 9	187, 31	494, 81	152, 25
		<b>6.0</b>	101, 16	334, 55	927, 152	529, 87
5	NCT04333732	6.7	1.2, 0.2	2.8, 0.5	2.3, 0.4	1.0, 0.2
6	NCT04333732	6.7	1.3, 0.2	2.8, 0.5	3.7, 0.6	4.3, 0.7
		6.0	16, 2.5	49, 8.0	85, 14	108, 18
		<b>6.0</b>	29, 4.7	87, 14	163, 27	261, 43

Bold values indicate when renal impairment is also being accounted for.

CQ, chloroquine; EC<sub>90</sub>, effective concentration 90%; FDA, US Food and Drug Administration; R<sub>EC50</sub>, ratio of the simulated lung mass unbound concentration to the reported lowest half-maximal effective concentration (EC<sub>50</sub>) value (1.13 µM) against severe acute respiratory syndrome coronavirus-2 virus in Vero E6 cells with 48-hour incubation time; WHO, World Health Organization. R<sub>EC90</sub>, ratio of the simulated lung mass unbound concentration to EC<sub>90</sub> value (6.9 µM) against SARS-CoV-2 virus in Vero E6 cells.

minimum cited EC<sub>50</sub> value for inhibition of SARS-CoV-2 on the third day of dosing (Figure 4) but only the EC<sub>90</sub> value on the last day of dosing.

**Simulated plasma and lung exposure of AZ**

After a single oral dose of 500 mg AZ, predicted plasma C<sub>max</sub> and area under the curve (AUC) values were within 80–120%

of observed values (ref. 32; data not shown). Predicted C<sub>max</sub> values in the ELF and lungs were 1.39 and 7.36 µg/mL, respectively, which were consistent with observed values of 1.20 and 8.30 µg/mL, respectively. Based on C<sub>max</sub> values, predicted tissue to plasma ratios were 3.73 and 19.8 for ELF and lung tissue, respectively, which were again similar to observed values of 3.08 and 21.3. Concentration-time profiles for AZ in plasma and lungs (lung

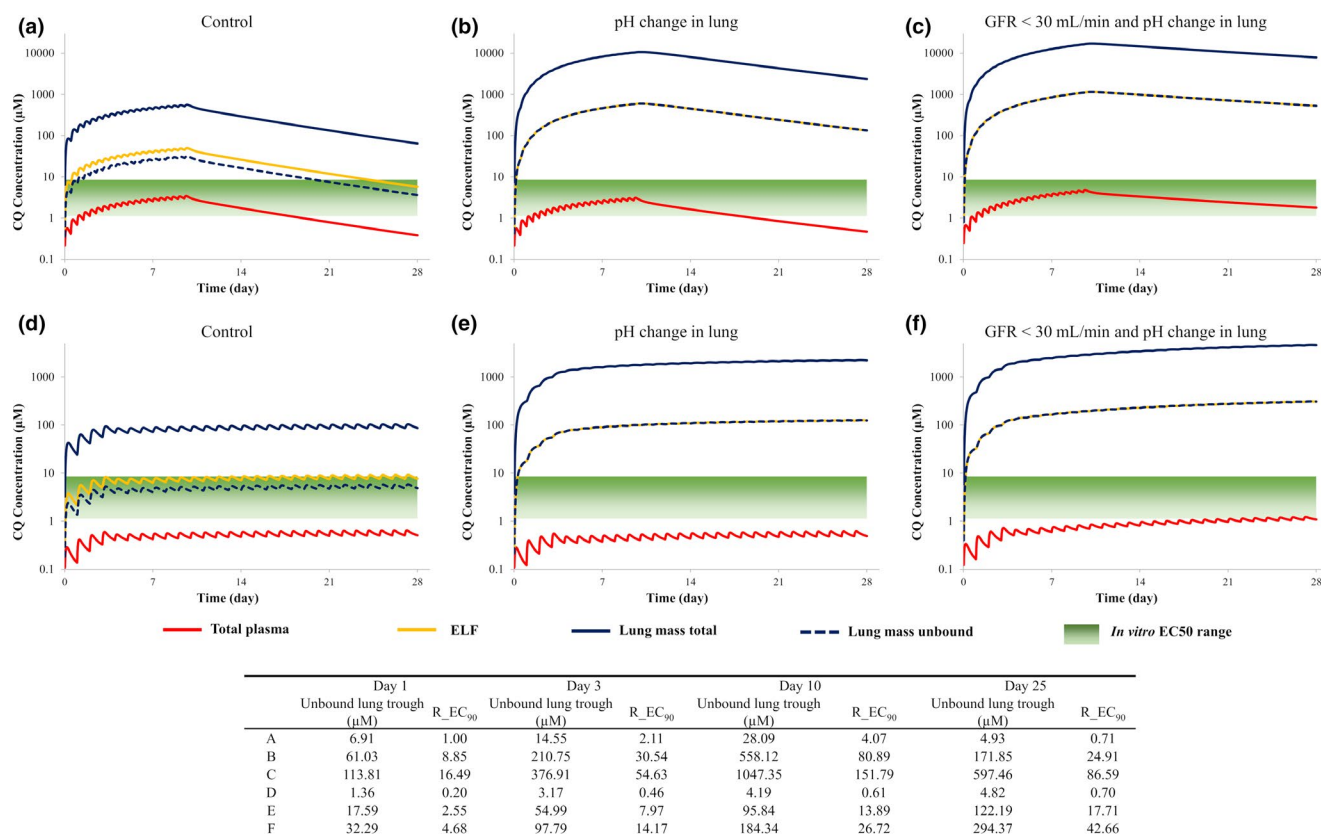


**Figure 3** The effect of a reduction in lung pH and renal impairment on the plasma and lung exposure of chloroquine (CQ) relative to *in vitro* half-maximal effective concentration ( $EC_{50}$ ) values for two dosing regimens. (a–c) There was 600 mg b.i.d. administered for 10 days (ClinicalTrials.gov Identifier: NCT04323527); (d–f) 300 mg q.d. for 4 days, followed by 150 mg q.d. (ClinicalTrials.gov Identifier: NCT04333732). Total plasma (red line), lung mass total (blue solid line), lung mass unbound (blue dashed line), epithelial lining fluid (ELF; yellow line) are shown. R<sub>EC90</sub>: Ratio of the simulated lung mass unbound concentration to effective concentration 90% ( $EC_{90}$ ) value (6.9 µM) against severe acute respiratory syndrome-coronavirus 2 virus in Vero E6 cells. GFR, glomerular filtration rate.

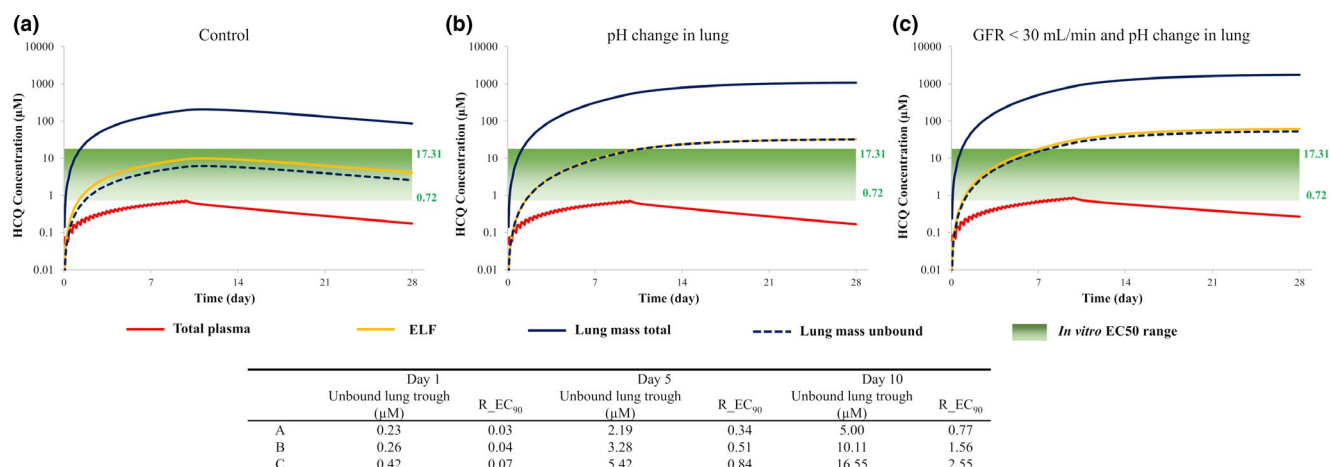


**Figure 4** Simulated plasma and lung concentrations of hydroxychloroquine (HCQ; 400 mg every 8 hours for 10 days) relative to *in vitro* half-maximal effective concentration ( $EC_{50}$ ) values (a) and the effect of reduced lung pH (b) and renal impairment (c). Total plasma (red line), lung mass total (blue solid line), lung mass unbound (blue dashed line), epithelial lining fluid (ELF; yellow line) are shown. R<sub>EC90</sub>: Ratio of the simulated lung mass unbound concentration to effective concentration 90% ( $EC_{90}$ ) value (6.48 µM) against severe acute respiratory syndrome-coronavirus 2 virus in Vero E6 cells. GFR, glomerular filtration rate.

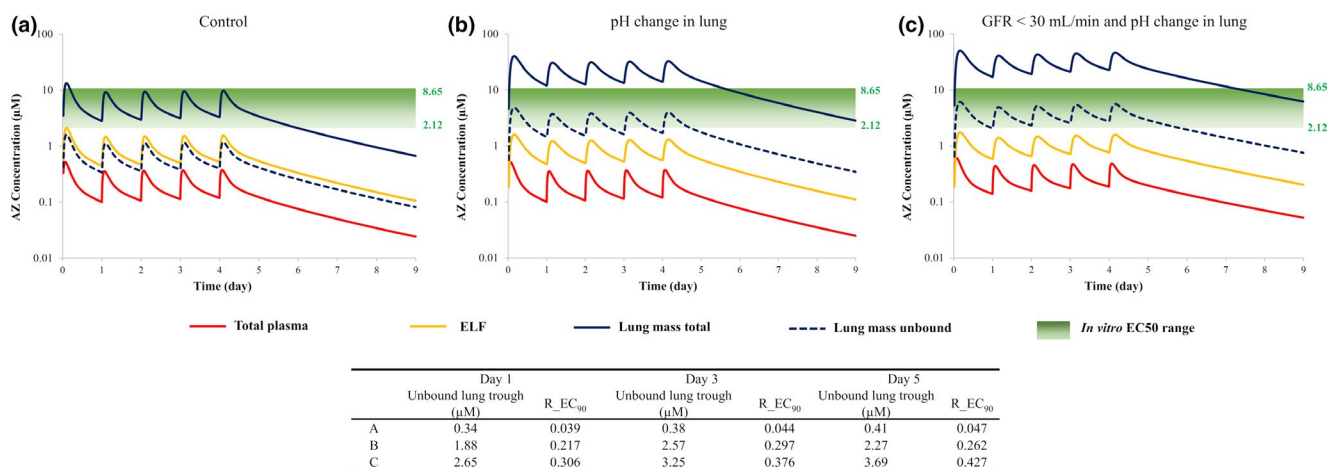


**Figure 5** Simulated plasma and lung concentrations of azithromycin (AZ; 500 mg on day 1 followed by 250 mg daily for 4 days) relative to *in vitro* half-maximal effective concentration (EC<sub>50</sub>) values (a) and the effect of reduced lung pH (b) and renal impairment (c). Total plasma (red line), lung mass total (blue solid line), lung mass unbound (blue dashed line), epithelial lining fluid (ELF; yellow line) are shown. R\_EC<sub>90</sub>: Ratio of the simulated lung mass unbound concentration to effective concentration 90% (EC<sub>90</sub>) value (8.65 µM) against severe acute respiratory syndrome-coronavirus 2 virus in Vero E6 cells. GFR, glomerular filtration rate.

tissue and ELF) after a single oral dose of 500 mg followed by 250 mg daily for 4 days are shown in **Figure 5**. A reduction in lung pH does not lead to a change in plasma exposure but a 2.7-fold increase in C<sub>max</sub> is expected in the lungs (12.4 vs. 33.5 µM). A 20% increase in plasma exposure is predicted in subjects with renal impairment and the C<sub>max</sub> in the lungs is further increased to 42.5 µM. Unbound lung concentrations of AZ do not attain the cited EC<sub>50</sub> or EC<sub>90</sub> values (**Figure 5**).

## DISCUSSION

In the current study, we sought to demonstrate that the accumulation of CQ, HCQ, and AZ in the lungs is sensitive to lung pH, a parameter, which could change significantly in patients as a consequence of having COVID-19. The degree of accumulation is largely dependent on drug-related parameters (log D, pK<sub>a</sub>, f<sub>u,plasma</sub>, and f<sub>u,mass</sub>) and the pH gradients maintained across the blood vessels and the lungs. This complex interplay of parameters is captured by the mechanistic multicompartment permeability limited lung model<sup>12</sup> and allowed us to investigate the effect of COVID-19 and associated comorbidities on the predicted concentrations of CQ, HCQ, and AZ in the lungs and plasma. A change in pH from 6.7 to 6 in the lungs, which is observed in respiratory disease, led to 20-fold, 4.0-fold, and 2.7-fold increases in lung exposure of CQ, HCQ, and AZ, respectively, due to an increase in ionization of the drugs. Furthermore, the high concentrations of CQ and HCQ in lung tissue were sustained long after administration of the drugs had stopped. A significant number of patients with COVID-19 present with kidney failure.<sup>7</sup> Our simulations indicate that renal impairment (plus lung pH reduction) caused 30-fold, 8.0-fold, and 3.4-fold increases in lung exposures for CQ, HCQ, and AZ, respectively. Accompanying increases (20–30%) in systemic exposure were relatively small indicating standard pharmacokinetic measurements are unlikely to inform on drug concentration at the site of action.

One of the limitations of this study is that predicted baseline concentrations of the drugs in the lungs could only be verified for AZ. Clinical data for AZ were characterized in plasma, ELF, alveolar macrophages, and lung tissue itself.<sup>32</sup> For CQ and HCQ, K<sub>p</sub> values for the lungs derived from rat data provided some level of verification. The lung model has been applied previously, with reasonable success, to predict the lung exposure of at least seven drugs used in the treatment of tuberculosis.<sup>12</sup> However, future studies that characterize CQ and HCQ concentrations in ELF, plasma, alveolar macrophage, and/or bronchial tissue are warranted. In addition, robust *in vitro* data relating to the permeability of the drugs across the lungs are required to enhance the PBPK models for these drugs.

It is assumed that drug efficacy at the site of action is determined by the unbound drug in the tissue. The unbound fraction in the lungs was not available for these drugs and, therefore, had to be predicted based on physicochemical properties.<sup>19</sup> Predicted f<sub>u,mass</sub> values (in the lungs) were 0.056, 0.030, and 0.12 for CQ, HCQ, and AZ, respectively. These are markedly lower than the measured f<sub>u</sub> values in plasma given by 0.4, 0.50, and 0.69, respectively. When f<sub>u,mass</sub> values are applied to the total lung concentrations, most of the dosage regimens that were simulated for CQ, HCQ, and AZ seemed to attain concentrations that were comparable with the *in vitro* derived EC<sub>50</sub> values, despite the EC<sub>50</sub> values being highly variable for each compound. When compared against the EC<sub>90</sub> values, it appears that for HCQ, the dosage regimen investigated in the French study (155 mg base three times a day for 10 days)<sup>3</sup> was not able to attain lung exposures in this target range, a finding which was in agreement with Arnold and Buckner.<sup>11</sup> Yao *et al.*<sup>2</sup> reported that, based on their PBPK modeling results, HCQ (a loading dose of 310 mg base given twice on day 1 followed by 155 mg twice daily for 4 days) should be recommended for treatment of COVID-19, as this dosage regimen was likely to attain high enough concentrations in the lungs to inhibit the SARS-CoV-2 virus.

For CQ, the potential 20-fold increase in lung exposure in patients with COVID-19 relative to healthy subjects, led to predicted unbound concentrations in the lungs that were higher than the EC<sub>90</sub> from day 1 even for one of the more conservative dosage regimens (300 mg for days 1 to 4, followed by 150 mg q.d.). Given the uncertainty associated with the predicted  $f_{u, \text{mass}}$  values and their impact on dose selection, appropriate *in vitro* studies to measure tissue binding in lung homogenate should be conducted to lend more weight to the predictions. It may also be pertinent to use EC<sub>90</sub> values derived from measured intracellular concentrations rather than those added to the cell culture media *in vitro*.<sup>33</sup> As uptake of both CQ and HCQ is sensitive to pH, it cannot simply be assumed that uptake into cells *in vitro* reflects accumulation of the drugs in the lungs.<sup>33</sup>

Last, but certainly not least, concerns relating to CQ and HCQ toxicity should also help inform dose selection. There are an increasing number of reports of associated QT prolongation and it is possible that patients with COVID-19 may be more susceptible to CQ and HCQ toxicity.<sup>34</sup> Going forward, efforts should be made to link the exposure of CQ and HCQ in the heart with markers of QT prolongation, such as the EC<sub>50</sub> data derived for inhibition of cardiac ion channels<sup>35</sup> to better understand margins of cardiac safety.

Although it is important to acknowledge the limitations described and collect more clinical data to verify drug exposures in the lungs, as highlighted by Arnold and Buckner,<sup>11</sup> our study does show that there is a place for PBPK modeling to inform the advancement of HQ and CQ and AZ as potential candidates for treatment of COVID-19. Furthermore, the strategy taken here may be useful to assess and prioritize other drugs that are potential candidates for repurposing.

#### SUPPORTING INFORMATION

Supplementary information accompanies this paper on the *Clinical Pharmacology & Therapeutics* website ([www.cpt-journal.com](http://www.cpt-journal.com)).

#### ACKNOWLEDGMENTS

The authors would like to acknowledge The Bill & Melinda Gates Foundation for funding the development of the original chloroquine model. We would like to thank Dr. Ping Zhao for his review of the manuscript and Eleanor Savill for her assistance with manuscript preparation.

#### CONFLICT OF INTEREST

All authors are paid employees of Certara UK Limited (Simcyp Division) or Certara Inc.

#### FUNDING

No funding was received for this work.

#### AUTHOR CONTRIBUTIONS

K.R.Y., M.Z., X.P., L.A., A.K., and H.M.J. wrote the manuscript. K.R.Y., M.Z., X.P., D.W., L.A., H.M.J., and A.K. designed the research. K.R.Y., M.Z., X.P., D.W., L.A., H.M.J., and A.K. performed the research. K.R.Y., M.Z., X.P., D.W., L.A., H.M.J., and A.K. analyzed the data.

© 2020 The Authors. *Clinical Pharmacology & Therapeutics* published by Wiley Periodicals LLC. on behalf of American Society for Clinical Pharmacology and Therapeutics.

This is an open access article under the terms of the Creative Commons Attribution-NonCommercial License, which permits use, distribution and reproduction in any medium, provided the original work is properly cited and is not used for commercial purposes.

- Gao, J., Tian, Z. & Yang, X. Breakthrough: Chloroquine phosphate has shown apparent efficacy in treatment of COVID-19 associated pneumonia in clinical studies. *Biosci. Trends* **14**, 72–73 (2020).
- Yao, X. *et al.* In vitro antiviral activity and projection of optimized dosing design of hydroxychloroquine for the treatment of severe acute respiratory syndrome coronavirus 2 (SARS-CoV-2). *Clin. Infect. Dis.* <https://doi.org/10.1093/cid/ciaa237>. [e-pub ahead of print].
- Gautret, P. *et al.* Hydroxychloroquine and azithromycin as a treatment of COVID-19: results of an open-label non-randomized clinical trial. *Int. J. Antimicrob. Agents* <https://doi.org/10.1016/j.ijantimicag.2020.105949>. [e-pub ahead of print].
- Hallifax, D. & Houston, J.B. Saturable uptake of lipophilic amine drugs into isolated hepatocytes: mechanisms and consequences for quantitative clearance prediction. *Drug Metab. Disposition* **35**, 1325–1332 (2007).
- Collins, K.P., Jackson, K.M. & Gustafson, D.L. Hydroxychloroquine: a physiologically-based pharmacokinetic model in the context of cancer-related autophagy modulation. *J. Pharmacol. Exp. Ther.* **365**, 447–459 (2018).
- Cheng, Y. *et al.* Kidney impairment is associated with in-hospital death of COVID-19 patients. *Kidney Int.* **97**, 829–838 (2020).
- Pan, X.-W., Xu, D., Zhang, H., Zhou, W., Wang, L.-H. & Cui, X.-G. Identification of a potential mechanism of acute kidney injury during the covid-19 outbreak: a study based on single-cell transcriptome analysis. *Intensive Care Med.* **46**, 1114–1116 (2020).
- Jones, H. & Rowland-Yeo, K. Basic concepts in physiologically based pharmacokinetic modeling in drug discovery and development. *CPT Pharmacometrics Syst. Pharmacol.* **2**, 1–12 (2013).
- Rowland Yeo, K., Aarabi, M., Jamei, M. & Rostami-Hodjegan, A. Modeling and predicting drug pharmacokinetics in patients with renal impairment. *Expert Rev. Clin. Pharmacol.* **4**, 261–274 (2011).
- Johnson, T.N., Boussey, K., Rowland-Yeo, K., Tucker, G.T. & Rostami-Hodjegan, A. A semi-mechanistic model to predict the effects of liver cirrhosis on drug clearance. *Clin. Pharmacokinet.* **49**, 189–206 (2010).
- Arnold, S.L. & Buckner, F. Hydroxychloroquine for treatment of SARS-CoV-2 infection? Improving our confidence in a model-based approach to dose selection. *Clin. Transl. Sci.* **13**, 642–645 (2020).
- Gaohua, L. *et al.* Development of a multicompartment permeability-limited lung PBPK model and its application in predicting pulmonary pharmacokinetics of antituberculosis drugs. *CPT Pharmacometrics Syst. Pharmacol.* **4**, 605–613 (2015).
- Liu, J. *et al.* Hydroxychloroquine, a less toxic derivative of chloroquine, is effective in inhibiting SARS-CoV-2 infection in vitro. *Cell Discov.* **6**, 1–4 (2020).
- Touret, F. *et al.* In vitro screening of a FDA approved chemical library reveals potential inhibitors of SARS-CoV-2 replication. *bioRxiv*. <https://doi.org/10.1101/2020.04.03.023846>. [e-pub ahead of print].
- Wang, M. *et al.* Remdesivir and chloroquine effectively inhibit the recently emerged novel coronavirus (2019-nCoV) in vitro. *Cell Res.* **30**, 269–271 (2020).
- Johnson, T.N., Jamei, M. & Rowland-Yeo, K. How does in vivo biliary elimination of drugs change with age? Evidence from in vitro and clinical data using a systems pharmacology approach. *Drug Metab. Disposition* **44**, 1090–1098 (2016).
- Kiem, S. & Schentag, J.J. Interpretation of antibiotic concentration ratios measured in epithelial lining fluid. *Antimicrob. Agents Chemother.* **52**, 24–36 (2008).
- Jamei, M. *et al.* A mechanistic framework for in vitro–in vivo extrapolation of liver membrane transporters: prediction of drug–drug interaction between rosuvastatin and cyclosporine. *Clin. Pharmacokinet.* **53**, 73–87 (2014).

19. Rodgers, T., Leahy, D. & Rowland, M. Physiologically based pharmacokinetic modeling 1: predicting the tissue distribution of moderate-to-strong bases. *J. Pharm. Sci.* **94**, 1259–1276 (2005).
20. Katneni, K. et al. Using human plasma as an assay medium in Caco-2 studies improves mass balance for lipophilic compounds. *Pharm. Res.* **35**, 210 (2018).
21. Ferrari, V. & Cutler, D.J. Kinetics and thermodynamics of chloroquine and hydroxychloroquine transport across the human erythrocyte membrane. *Biochem. Pharmacol.* **41**, 23–30 (1991).
22. Nožinić, D., Milić, A., Mikac, L., Ralić, J., Padovan, J. & Antolović, R. Assessment of macrolide transport using PAMPA, Caco-2 and MDCKII-hMDR1 assays. *Croat. Chem. Acta* **83**, 323–331 (2010).
23. Fischer, H. & Widdicombe, J.H. Mechanisms of acid and base secretion by the airway epithelium. *J. Membr. Biol.* **211**, 139–150 (2006).
24. Gessner, C. et al. Exhaled breath condensate acidification in acute lung injury. *Respir. Med.* **97**, 1188–1194 (2003).
25. Effros, R.M. & Chinard, F.P. The in vivo pH of the extravascular space of the lung. *J. Clin. Invest.* **48**, 1983–1996 (1969).
26. Viasus, D. et al. Prognostic value of serum albumin levels in hospitalized adults with community-acquired pneumonia. *J. Infect.* **66**, 415–423 (2013).
27. Wi, Y., Kim, J. & Peck, K. Serum albumin level as a predictor of intensive respiratory or vasopressor support in influenza A (H1N1) virus infection. *Int. J. Clin. Pract.* **68**, 222–229 (2014).
28. Bohte, R., Mattie, H. & van den Broek, P.J. Levels of azithromycin and alpha-1 acid glycoprotein in serum in patients with community-acquired pneumonia. *Antimicrob. Agents Chemother.* **39**, 2801–2802 (1995).
29. Wan, J. et al. Inflammation inhibitors were remarkably up-regulated in plasma of severe acute respiratory syndrome patients at progressive phase. *Proteomics* **6**, 2886–2894 (2006).
30. McChesney, E., Fasco, M., Banks, W. & Kersch, T.B. The metabolism of chloroquine in man during and after repeated oral dosage. *J. Pharmacol. Exp. Ther.* **158**, 323–331 (1967).
31. Munster, T. et al. Hydroxychloroquine concentration–response relationships in patients with rheumatoid arthritis. *Arthritis Rheum.* **46**, 1460–1469 (2002).
32. Lucchi, M. et al. Pharmacokinetics of azithromycin in serum, bronchial washings, alveolar macrophages and lung tissue following a single oral dose of extended or immediate release formulations of azithromycin. *J. Antimicrob. Chemother.* **61**, 884–891 (2008).
33. Fan, J. et al. Connecting hydroxychloroquine in vitro antiviral activity to in vivo concentration for prediction of antiviral effect: a critical step in treating COVID-19 patients. *Clin. Infect. Dis.* <https://doi.org/10.1093/cid/ciaa623>. [e-pub ahead of print].
34. Giudicessi, J.R., Noseworthy, P.A., Friedman, P.A. & Ackerman, M.J. Urgent guidance for navigating and circumventing the QTc-prolonging and torsadogenic potential of possible pharmacotherapies for coronavirus disease 19 (COVID-19). *Mayo Clin. Proc.* **95**, 1213–1221 (2020).
35. Polak, S. et al. Quantitative approach for cardiac risk assessment and interpretation in tuberculosis drug development. *J. Pharmacokinet. Pharmacodyn.* **45**, 457–467 (2018).
36. Adelus, S. & Salako, L. Kinetics of the distribution and elimination of chloroquine in the rat. *Gen. Pharmacol.* **13**, 433–437 (1982).
37. Adelus, S. & Salako, L. Tissue and blood concentrations of chloroquine following chronic administration in the rat. *J. Pharm. Pharmacol.* **34**, 733–735 (1982).